Int J Thermophys (2007) 28:835–845
DOI 10.1007/s10765-007-0217-8

Theoretical Calculation of the Low-Density Transport Properties of Monatomic Silver Vapor

L. Biolsi · P. M. Holland

Published online: 9 August 2007

Abstract Calculations of low-density transport property collision integrals are used to obtain the high-temperature transport properties of silver atoms as a function of temperature. The collision integrals depend on the two-body interaction potentials between silver atoms in various electronic states. Contributions are included from the ground $X^1\Sigma_g^+$ and excited $^3\Sigma_u^+$ molecular electronic states of the silver dimer that dissociate to two ground-state silver atoms and from the excited $A^1\Sigma_u^+$ molecular state that dissociates to a ground state and an excited state silver atom. Spectroscopic constants are available for these three electronic states, and these spectroscopic constants have been used to determine the Hulburt–Hirschfelder (HH) potentials for these three states. The HH potential is perhaps the best general-purpose potential for representing atom–atom interactions. This potential depends only on the spectroscopic constants, and can be used to calculate the viscosity and diffusion collision integrals for the three molecular electronic states. The collision integrals are then degeneracy averaged over the three states. The heat capacity of silver atoms is also calculated at high temperatures. These results provide the information required to obtain the thermal conductivity, viscosity, and self-diffusion coefficients of silver atoms over a wide temperature range from the boiling point of silver to temperatures at which ionization becomes important.

L. Biolsi (✉)
Chemistry Department, University of Missouri-Rolla,
Rolla, MO 65401, USA
e-mail: louis@biolsi.com

P. M. Holland
Thorleaf Research Inc., 5552 Cathedral Oaks Road,
Santa Barbara, CA 93111-1406, USA

Keywords Diffusion · Silver atoms · Thermal conductivity · Transport properties · Viscosity

1 Introduction

Small clusters of silver atoms are of special interest since they may serve as a prototype for solid surfaces which have important catalytic properties in bulk [1] and as nanosilver surfaces [2]. Small silver clusters are also important in the formation of photographic images [3]. Recently, the thermodynamic properties of silver dimers, Ag_2, have been theoretically calculated [4], and this article is concerned with theoretical calculations of the transport properties of silver atoms, Ag; e.g., the viscosity, thermal conductivity, and diffusion coefficient. At low-density the viscosity, η, is given by [5]

$$\eta(\mu\text{Pa}\cdot\text{s}) = 2.669\frac{\sqrt{MT}}{\sigma^2\Omega^{(2,2)^*}} \tag{1}$$

the diffusion coefficient, D, is given by

$$D(\text{m}^2\cdot\text{s}^{-1}) = 2.594\times10^{-7}\frac{\sqrt{T^3/M}}{p\sigma^2\Omega^{(1,1)^*}} \tag{2}$$

the translational contribution to the thermal conductivity, λ_{tr}, is given by

$$\lambda_{\text{tr}}(\text{W}\cdot\text{m}^{-1}\cdot\text{K}^{-1}) = 8.322\times10^{-2}\frac{\sqrt{T/M}}{\sigma^2\Omega^{(2,2)^*}} \tag{3}$$

and the internal contribution to the thermal conductivity, λ_{int}, is given by [6,7]

$$\lambda_{\text{int}}(\text{W}\cdot\text{m}^{-1}\cdot\text{K}^{-1}) = 1.203\times10^4\frac{pD}{T}(C_p - 20.786) \tag{4}$$

where T is the temperature in K, M is the molar mass in g· mol^{-1}, p is the pressure in bar, C_p is the molar heat capacity at constant pressure in J· mol^{-1}· K^{-1}, and $\sigma^2\Omega^{(1,1)^*}$, and $\sigma^2\Omega^{(2,2)^*}$ are the diffusion and viscosity collision integrals in 10^{-20}Å^2, respectively, determined by the interaction between two Ag atoms as they "follow" a particular electronic potential energy curve. Equation (4) is valid subject to the assumption that the transport of internal energy is due only to a diffusion mechanism [6,7].

2 Interaction Potentials

Theoretical calculations of the transport collision integrals depend on the algebraic expression for the potential energy that is used to represent the Ag–Ag interactions. The Hulburt–Hirschfelder potential [8,9] is used to represent the interactions for these calculations. It has the reduced form,

$$V^*(R^*) = \text{e}^{-2Ax} - 2\text{e}^{-Ax} + Bx^3\,(1+Gx)\,\text{e}^{-2Ax} \tag{5}$$

where

$$A = \frac{\omega_e}{2\sqrt{B_e \varepsilon}}, \quad B = cA^3, \quad G = bA, \quad d = \frac{R_e}{\sigma}$$

$$c = 1 + a_1 \sqrt{\frac{\varepsilon}{a_0}}, \quad b = 2 - \frac{7/12 - \varepsilon a_2/a_0}{c}$$

$$a_0 = \frac{\omega_e^2}{4B_e}, \quad a_1 = -1 - \frac{\alpha_e \omega_e}{6B_e^2}, \quad a_2 = \frac{5}{4}a_1^2 - \frac{2\omega_e \chi_e}{3B_e}$$

$$V^* = \frac{V}{\varepsilon}, \quad R^* = \frac{R}{\sigma}, \quad x = \frac{R^*}{d} - 1$$

Also, R is the internuclear separation between the two Ag atoms, V is the potential energy, σ is the effective rigid sphere diameter, i.e., the value of R at which V goes to zero, ε is the depth of the potential energy well, R_e is the value of R at $V = \varepsilon$, ω_e is the fundamental vibrational frequency, $\omega_e \chi_e$ is the anharmonicity constant, B_e is the rotational constant, and α_e is the vibration-rotation coupling constant. Thus, this potential depends only on the spectroscopic constants. It is the most accurate available general purpose potential for representing atom–atom interactions with an attractive minimum in the potential [10–14], and it usually gives excellent agreement with experimental Rydberg–Klein–Rees (RKR) potential energy curves for atom–atom and atom–ion interactions [10,12,15–17] without the need for adjustable parameters. It also often reproduces the local maxima sometimes found at larger interatomic separations [18–22]. More accurate potentials can probably be obtained for the electronic states of Ag_2 as has been done for a number of other diatomic species. However, such potentials usually involve extensive parameterization.

HH potential energy curves are obtained for three low-lying electronic states of Ag_2: the ground $X^1\Sigma_g^+$ state and the excited $^3\Sigma_u^+$ and $A^1\Sigma_u^+$ states. The first two states dissociate to two ground-state ^{2}S Ag atoms, but the $A^1\Sigma_u^+$ state dissociates to one ^{2}S Ag atom and an excited state ^{2}P Ag atom. The experimental spectroscopic information required for the HH potential is available [23–25] for the $X^1\Sigma_g^+$ and the $A^1\Sigma_u^+$ states. However, there is no experimental spectroscopic information for the $^3\Sigma_u^+$ state since it is weakly bound. The theoretical calculations of Zhang and Balasubramanian [26] have been used for T_e, the energy at the bottom of the potential energy well, and for ω_e and B_e. This provides enough information to use the Levine potential [27–29], but it is also possible to estimate $\omega_e \chi_e$ and α_e [26–28]. Thus, an HH potential can be estimated for this state. The spectroscopic constants used for these calculations are given in Table 1, and the four potential energy curves (two curves for the $^3\Sigma_u^+$ state) are shown in Fig. 1. The two curves for the $^3\Sigma_u^+$ state are similar.

The normal boiling point of silver [30] is 2,485 K and, if only the ground state is occupied, ionization becomes important at about 30,000 K (where 5% of the silver

Table 1 Spectroscopic constants for Ag_2

Constants	$X^1\Sigma_g^+$	$^3\Sigma_u^+$	$A^1\Sigma_u^+$
$\omega_e(cm^{-1})$	192.4[a]	34[d]	154.6[a]
$\omega_e\chi_e(cm^{-1})$	0.643[a]	0.1122[e]	0.587[b]
B_e (cm^{-1})	0.04878[b]	0.026731[d]	0.044331[b]
$\alpha_e(cm^{-1})$	0.0001952[b]	0.0001439[e]	0.000215[b]
R_e(Å)	2.53096[b]	3.419[d]	2.6549[b]
D_e(eV)	1.65[c]	0.28[d]	2.46[f]

[a] From Ref. 23
[b] From Ref. 24
[c] From Ref. 25
[d] From Ref. 26
[e] Estimated from procedures in Refs. 27–29
[f] Calculated from T_e in Ref. 23

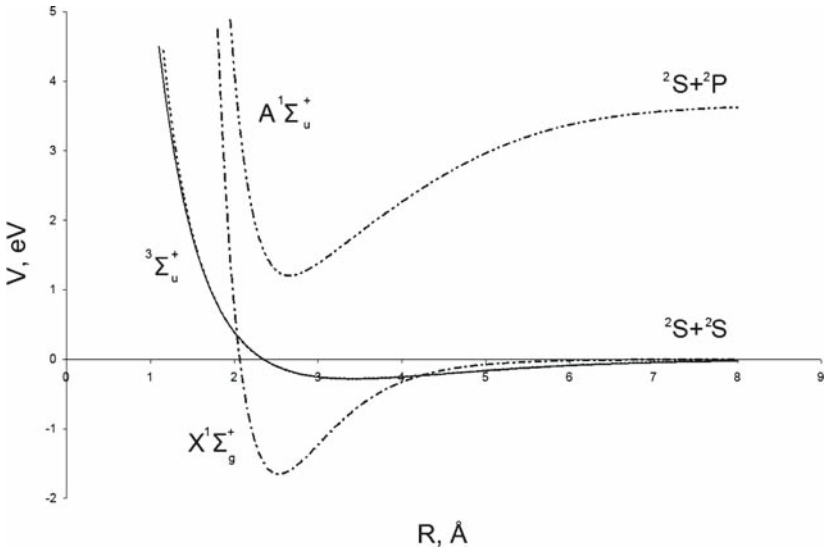

Fig. 1 Plot of the electronic potential energy, V, versus the separation of the two Ag atoms, R; HH potential for the Ground $X^1\Sigma_g^+$ state (—· — · — ·—); HH potential for the $^3\Sigma_u^+$ state (—); Levine potential for the $^3\Sigma_u^+$ state (····); HH potential for the $A^1\Sigma_u^+$ state (—·· — ··—)

atoms at equilibrium are ionized). Thus, calculations are presented here from 2,000 to 30,000 K. At equilibrium at 5,000 K, only 1% of the Ag_2 molecules are in the $A^1\Sigma_u^+$ state, 2% of the molecules are in this state at 10,000 K, but 17% of the molecules are in this state at 30,000 K. Thus, collision integrals for this state should be included at higher temperatures.

3 Ideal-Gas Heat Capacity of Silver Atoms

The ideal-gas heat capacity of silver atoms is not given in the JANAF Thermochemical Tables [31]. However, the information about atomic energy levels required to estimate the heat capacity at relatively high temperatures is available [32,33]. This information is required to calculate the contribution to the thermal conductivity from internal (electronic) degrees of freedom. The procedure for doing this is discussed by Downey [34].

The Ag ground state has the electron configuration $1s^2 2s^2 2p^6 3s^2 3p^6 3d^{10} 4s^2 4p^6 4d^{10} 5s$. The electronic partition function, Q_{el}, is given by

$$Q_{el} = \sum_n g_n e^{-\varepsilon_n / kT}$$

where n labels the principal quantum number, g_n is the electronic degeneracy, ε_n is the electronic energy, and k is Boltzmann's constant. At low temperatures, only the ground state need be included in the summation. However, since there are an infinite number of energy levels between the lowest atomic energy level ($n = 5$ in this case) and the continuum at the ionization limit, more than one term must be included in the sum at high temperatures.

The Downey procedure selects terms involving the excitation of only the most easily excitable electron [34], in this case the 5s electron. The first question to be addressed is the number of n values that contribute terms to the partition function at a given temperature. Downey uses Bethe's [35] criterion;

$$n_{max} = 2.461 T^{1/6}$$

For silver, n_{max} is 9 at 2,000 K and 14 at 30,000 K. Thus, at 2,000 K, there should be Boltzmann factors for $n = 5$–9 included in the partition function. Downey groups these as follows: the one excited electron $n = 5$ contributions are

$$5p,\ 5d,\ 5f,\ 5g,\ 4f,\ 4d^9 5s^2,\ 4d^9 5s5p,\ 4d^9 5s5d$$

The total number for the degeneracies of these states is 394. Experimental energy level information is available [32,33] for all the states except the $4d^9 5s5d$ which has a total degeneracy of 200. Downey [34] suggests estimating the Boltzmann factor for states without an experimentally determined energy level by using the highest experimentally available energy (for the $4d^9 5s5p$ state in this case). Thus, it is clear that, even for the lowest contributing value of n, approximations must be made. The excited $n = 6$ contributions are

$$6s,\ 6p,\ 6d,\ 6f,\ 6g,\ 6h$$

with a total degeneracy of 72. No information is available for the 6g and 6h states with a total degeneracy of 40 so the 6f energy level is used for these states. The excited

$n = 7$ contributions are

$$7s, 7p, 7d, 7f, 7g, 7h, 7i$$

with a total degeneracy of 98. No information is available for the 7f, 7g, 7h, and 7i states with a total degeneracy of 80. Thus, the 7d experimental energy is used. The excited $n = 8$ contributions are

$$8s, 8p, 8d, 8f, 8g, 8h, 8i, 8j$$

with a total degeneracy of 128. Since no information is available for the 8f, 8g, 8h, 8i, and 8j states with a total degeneracy of 110, the 8d experimental energy is used. The excited $n = 9$ contributions are

$$9s, 9p, 9d, 9f, 9g, 9h, 9i, 9j, 9k$$

with a total degeneracy of 162. No information is available for the 9f, 9g, 9h, 9i, 9j, and 9k states with a total degeneracy of 144, and thus, the 9d experimental energy is used.

This procedure has been described in some detail so that the approximations used in this work are clear. However, since the energy levels become more closely spaced as the value of n increases, using the highest available energy for the missing states is not as bad an approximation as it might appear; e.g., the 9f, 9g, 9h, 9i, 9j, and 9k states have unknown energies that are "close" to the experimental energy of the 9d energy level.

As the temperature increases, Boltzmann factors for higher values of n should be included in Q_{el}. The highest value of n for which experimental energy levels are available [32] is $n = 12$. Since the Bethe [35] criterion indicates that contributions from $n = 13$ should be included at 20,000 K, the heat capacity is not calculated above 15,000 K. For $n = 12$, the contributions are

$$12s, 12p, 12d, 12f, 12h, 12i, 12j, 12k, 12\ell, 12m, 12n$$

with a total degeneracy of 288. Experimental energy levels are only available for the 12s and 12d states so the Boltzmann factors for the other states, with a total degeneracy of 276, are approximated with the 12d energy. This appears to be a severe approximation but the 12s and 12d energy levels, at about 60,000 cm^{-1}, are separated by only 433 cm^{-1} which is less than a 1% difference in energy.

Indeed, the 11s and 12d energy levels are separated by less than 900 cm^{-1}. The energy levels are indeed quite close together at high values of n. Since the ionization limit is 61106.45 cm^{-1} [33], it is tempting to take an approximate value, e.g., perhaps 60,000 cm^{-1}, and estimate the Boltzmann factors for $n > 12$. However, that has not been done.

The values of C_p^o of gas-phase silver atoms from 2,000 to 15,000 K are given in Table 2. The reliability of these values decreases as T increases. These results are consistent with the previous result [36] that C_p^o is 20.786 $\mathrm{J \cdot mol^{-1} \cdot K^{-1}}$ (a translational

Table 2 Heat capacity, C_p^o, Of Ag atoms

T (K)	C_p^o(J· mol^{-1}· K^{-1})	T(K)	C_p^o(J· mol^{-1}· K^{-1})
2000	20.7863	8000	42.1322
2500	20.7867	9000	62.2620
3000	20.7920	10, 000	85.3035
3500	20.8200	11, 000	109.2295
4000	20.9115	12, 000	110.0260
4500	21.1312	13, 000	98.9751
5000	21.5692	14, 000	83.5020
6000	23.6667	15, 000	68.7926
7000	29.6494		

contribution only) at 2,500 K. The heat capacity rises to a maximum; the rise is rapid from ∼8000 to 11,000 K which is the range at which low-lying and well-separated electronic states begin to be significantly populated. At higher temperatures, the heat capacity decreases since energy levels at higher values of n are quite close together and thus the ability of the atom to adsorb heat as the temperature increases is reduced.

4 Transport Properties

The program of Rainwater et al. [37] is used to calculate the collision integrals for each of the three molecular electronic potential energy curves. These must then be degeneracy averaged [38]. If only the two molecular states that dissociate to ground-state atoms were involved, the degeneracy averaged result would be

$$\sigma^2\Omega^{(a,b)^*}(DA) = \frac{1}{4}\sigma^2\Omega^{(a,b)^*}(X^1\Sigma_g^+) + \frac{3}{4}\sigma^2\Omega^{(a,b)^*}(^3\Sigma_u^+)$$

However, the inclusion of the $A^1\Sigma_u^+$ state complicates the degeneracy averaging. The degeneracies of the $X^1\Sigma_g^+$, $^3\Sigma_u^+$, and $A^1\Sigma_u^+$ are 1, 3, and 1, respectively. However, the $A^1\Sigma_u^+$ state dissociates to a ^{2}S and a ^{2}P atom. These atomic interactions form Σ and Π states with a total degeneracy [26] of 24. The only two such states for which there is experimental information are the $A^1\Sigma_u^+$ state [24,25] and the $^1\Pi_u$ state [39]. However, the $A^1\Sigma_u^+$ state is the lowest (most tightly bound) of these states while the $^1\Pi_u$ state has a very shallow minimum at higher energies [26] than for several other states in this group, states for which there are no experimental spectroscopic constants. Thus, this state has been ignored in these calculations.

The degeneracy averaged cross sections over the three molecular states are given by

$$\sigma^2\Omega^{(a,b)^*}(DA) = \frac{1}{4}\sigma^2\Omega^{(a,b)^*}(X^1\Sigma_g^+) + \frac{3}{4}\sigma^2\Omega^{(a,b)^*}(^3\Sigma_u^+) +$$

Table 3 Degeneracy averaged viscosity collision integrals for Ag atoms

T(K)	$\sigma^2\Omega^{(2,2)^*}$(Å^2)	T(K)	$\sigma^2\Omega^{(2,2)^*}$(Å^2)
2000	22.9383	20,000	3.9878
5000	10.8494	25,000	3.4206
10,000	6.5511	30,000	3.0269
15,000	4.8840		

$$\frac{1}{24}\sigma^2\Omega^{(a,b)^*}(A^1\Sigma_u^+)\mathrm{e}^{-5.8704\times10^{-19}\mathrm{J}/kT}$$

where 5.8704×10^{-19} J is the energy of the ^{2}P atom [33]. This expression is based on the assumption that the interacting atoms are at local equilibrium which is reasonable since the transport properties are nearly equilibrium properties, i.e., the gradients in composition, energy, and momentum are small [40]. Some degeneracy averaged viscosity cross sections are given in Table 3.

Calculation of the diffusion coefficient is more complicated. When the dissociation products are in different states such as dissociation to Ag atoms in the ^{2}S and ^{2}P states, it is the cross section for excitation exchange, e.g.,

$$\mathrm{Ag}(^2\mathrm{S}) + \mathrm{Ag}(^2\mathrm{P}) \rightarrow \mathrm{Ag}(^2\mathrm{P}) + \mathrm{Ag}(^2\mathrm{S})$$

that determines $\sigma^2\Omega^{(a,b)^*}$ for odd a [37]. Thus, the last term in the preceding expression should be replaced by

$$\frac{1}{12}(\text{excitation exchange cross section})\mathrm{e}^{-5.8704\times10^{-19}\mathrm{J}/(kT)}$$

for the diffusion process since the diffusion cross section is twice the exchange cross section [38].

In this case, the charge exchange cross section is related to coupling between the $\mathrm{A}^1\Sigma_\mathrm{u}^+$ state and the $^1\Sigma_\mathrm{g}^+$ state that dissociates to the same products. The exchange cross section can be related to the difference in potential energy between these states [41]. However, the potential energy for the $^1\Sigma_\mathrm{g}^+$ state is not available. Thus, the diffusion coefficient is not calculated above 15,000 K (the percentage of atoms in the $\mathrm{A}^1\Sigma_\mathrm{u}^+$ state at 15,000 K is about 5%). Results for the transport properties are given in Table 4. The table shows that $\lambda_{\mathrm{int}} > \lambda_{\mathrm{tr}}$ at higher temperatures since well separated energy levels are being populated at these temperatures. However, the differences decrease at the highest temperatures since the electronic energy levels are starting to "saturate."

5 Discussion

Neither experimental nor theoretical results for the transport properties of Ag atoms are available. Thus, a direct assessment of the accuracy of these results is not possible. The most important source of error is in the HH potentials used for the calculations,

Table 4 Transport Properties of Silver Atoms at Low Density

T(K)	$\eta(\mu\text{Pa}\cdot\text{s})$	$\lambda_{tr}(\text{mW}\cdot\text{m}^{-1}\cdot\text{K}^{-1})$	$\lambda_{int}(\text{mW}\cdot\text{m}^{-1}\cdot\text{K}^{-1})$	$D(10^{-4}\text{m}^2\cdot\text{s}^{-1})$
2000	54.044	15.622	0	1.081
2500	73.380	21.211	0.001	1.836
3000	93.852	27.129	0.007	2.817
3500	114.975	33.235	0.048	4.039
4000	136.506	39.458	0.210	5.501
4500	159.391	45.784	0.674	7.217
5000	180.665	52.223	1.756	9.198
6000	226.247	65.399	8.059	13.769
7000	273.285	78.995	30.738	19.915
8000	321.824	93.026	87.946	27.039
9000	371.892	107.499	198.991	35.422
10,000	423.137	122.311	354.741	45.105
11,000	475.743	137.518	549.881	56.104
12,000	528.930	152.892	621.242	68.530
13,000	583.715	168.728	602.673	82.201
14,000	639.031	184.717	531.568	97.343
15,000	695.129	200.933	444.381	113.904
20,000	983.053	284.160		
25,000	1281.336	370.381		
30,000	1586.200	458.504		

particularly for the $^3\Sigma_u^+$ state for which estimated spectroscopic constants were used. The authors have recently calculated [4] the heat capacity of the silver dimer, Ag_2, using a calculational procedure based on virial coefficients [42] which depend on the same three HH potentials. These results were compared with the heat capacity obtained using the standard partition function method [43]. This is shown in Table 5. Agreement is very good at low and intermediate temperatures to about 2,000 K, and deviates at higher temperatures with the partition function results about 30–50% higher above 3,000 K. There is reason to believe that the deviations at high temperatures are not due to errors in the HH potential energy curves, but are mostly due to the exclusion of continuum states from the partition function calculation [4]. The continuum states are repulsive and change the sign on the virial coefficients from negative to positive. This reduces the heat capacity, and this effect is not included in most partition function calculations [4]. On the other hand, the good agreement at low and intermediate temperatures provides evidence that the three HH potentials represent the true potential energy curves with reasonable accuracy.

There is a general rule of thumb [44] that an error of a factor of two in the potential leads to an error of 20–40% in the transport collision integrals. The HH potentials used here are certainly in error by less than a factor of two. Previous comparisons of the calculation of the viscosity of monatomic lithium [45] and monatomic sodium [46], using HH potentials, with the experimental results for lithium [47,48] and sodium [49–51] show a difference of approximately 10% or less. We conclude that the error in the transport properties shown in Table 4 is no greater than 10%.

Table 5 Ideal-Gas Heat Capacity, C_p^o, of Ag_2 (in $J \cdot mol^{-1} \cdot K^{-1}$)

T(K)	Virial	P.F.[a]	T (K)	Virial	P.F.[a]
200	36.94	36.21	1500	39.94	38.11
300	37.37	36.85	1600	40.57	38.62
400	37.59	37.09	1700	41.34	39.34
500	37.74	37.21	1800	42.25	40.31
600	37.87	37.27	1900	43.27	41.53
700	38.00	37.31	2000	44.36	43.03
800	38.12	37.33	2500	49.47	53.65
900	38.26	37.35	3000	51.16	64.52
1000	38.40	37.37	3500	49.10	69.45
1100	38.57	37.40	4000	45.28	68.03
1200	38.78	37.46	4500	41.29	63.40
1300	39.06	37.57	5000	37.85	58.23
1400	39.44	38.11			

[a] Partition function method

References

1. R. Romero, A. Mazuelos, I. Palencia, F. Carranza, Hydrometallurgy **70**, 205 (2003)
2. Z. Qu, W. Huang, M. Cheng, X. Bao, J. Phys. Chem. B **109**, 15842 (2005)
3. M.R.V. Sayhun, Phot. Sci. Eng. **22**, 317 (1978)
4. M.L. Biolsi, L. Biolsi, P.M. Holland, Paper #368. 228th Nat. Meeting (American Chemical Society, Philadelphia, 2004)
5. J.O. Hirschfelder, C.F. Curtiss, R.B. Bird, *Molecular Theory of Gases and Liquids, Chap. 8* (Wiley, New York, 1954)
6. E.A. Mason, L. Monchick, J. Chem. Phys. **36**, 1622 (1962)
7. J.T. Vanderslice, J.T.S. Weissman, E.A. Mason, R.J. Fallon, Phys. Fluids **5**, 155 (1962)
8. H.M. Hulburt, J.O. Hirschfelder, J. Chem. Phys. **9**, 61 (1941)
9. H.M. Hulburt, J.O. Hirschfelder, J. Chem. Phys. **35**, 1901 (1961)
10. D. Steele, E.R. Lippincott, J.T. Vanderslice, Rev. Mod. Phys. **34**, 239 (1962)
11. J.T. Vanderslice, E.A. Mason, W.G. Maisch, J. Chem. Phys. **32**, 515 (1960)
12. P.H. Krupenie, J. Phys. Chem. Ref. Data **1**, 423 (1972)
13. G.C. Lie, E. Clementi, J. Chem. Phys. **60**, 1288 (1974)
14. G. Das, A.C. Wahl, J. Chem. Phys. **44**, 87 (1966)
15. A. Lofthus, P.H. Krupenie, J. Phys. Chem. Ref. Data **6**, 113 (1977)
16. J.T. Vanderslice, E.A. Mason, W.G. Maisch, E.R. Lippincott, J. Chem. Phys. **33**, 614 (1960)
17. L. Biolsi, P.M. Holland, in *Progress in Astronautics and Aeronautics: Thermophysical Aspects of Re-entry Flows*, vol. **103**, ed. by J.N. Moss, C.D. Scott (AIAA, New York, 1986), pp. 261–278
18. L. Biolsi, J.C. Rainwater, P.M. Holland, J. Chem. Phys. **77**, 448 (1982)
19. G. Herzberg, *Molecular Spectra and Molecular Structure, I Spectra of Diatomic Molecules* (Van Nostrand, New York, 1950), pp. 425–430
20. R.S. Mulliken, J. Phys. Chem. **41**, 5 (1937)
21. J.C. Brown, F.A. Matsen, Adv. Chem. Phys. **23**, 161 (1973)
22. P.F. Fougere, R.K. Nesbet, J. Chem. Phys. **44**, 285 (1966)
23. K.P. Huber, G. Herzberg, *Molecular Spectra and Molecular Structure, IV Constants of Diatomic Molecules* (Van Nostrand Reinhold, New York, 1979), p. 8
24. B. Simard, P.A. Hackett, Chem. Phys. Lett. **186**, 415 (1991)
25. J.R. Lombardi, B. Davis, Chem. Rev. **102**, 2431 (2002)
26. H. Zhang, K. Balasubramanian, J. Chem. Phys. **98**, 7092 (1993)
27. I.N. Levine, J. Chem. Phys. **45**, 827 (1966)
28. H.W. Woolley, J. Chem. Phys. **37**, 1307 (1962)
29. Y.P. Varshni, R.C. Shukla, J. Chem. Phys. **40**, 250 (1964)

30. R.C. Weast (ed.), *Handbook of Physics and Chemistry*, 51st edn. (The Chemical Rubber Company, Cleveland, 1970), p. D-142
31. M.W. Chase Jr. (ed.), *NIST-JANAF Thermochemical Tables*, 4th edn., Part 1 (NIST, Washington, D.C, 1998)
32. C.E. Moore, *Atomic Energy Levels*, vol. III (NSRDS-NBS 35, Washington, DC, 1971), pp. 48–49
33. http://physics.nist.gov/PhysRefData/Handbook/Tables/silvertable1.htm
34. J.R. Downey Jr., The Dow Chemical Company, AFOSR-TR-0960, Contract #F44620-71-1-0048 (1978)
35. H. Bethe, Office of Scientific Research and Development Report #369 (1942)
36. I. Barin (ed.), *Thermochemical Data of Pure Substances*, Part I (VCH Pubs., Weinham, Germany, 1989), p. 2
37. J.C. Rainwater, P.M. Holland, L. Biolsi, J. Chem. Phys. **77**, 434 (1982)
38. E.A. Mason, J.T. Vanderslice, J.M. Yos, Phys. Fluids **6**, 688 (1959)
39. V. Beutel, M. Kuhn, W. Demtroder, J. Mol. Spectros. **155**, 343 (1992)
40. L. Biolsi, P.M. Holland, Int. J. Thermophys. **25**, 1063 (2004)
41. C. Nyeland, E.A. Mason, Phys. Fluids **10**, 985 (1967)
42. H.W. Woolley, J. Chem. Phys. **21**, 236 (1953)
43. D.A. McQuarrie, *Statistical Thermodynamics*, Chaps. 2, 6 (Harper & Row, New York, 1973)
44. P.H. Krupenie, E.A. Mason, J.T. Vanderslice, J. Chem. Phys. **39**, 2399 (1963)
45. P.M. Holland, L. Biolsi, J. Chem. Phys. **85**, 4011 (1986)
46. P.M. Holland, L. Biolsi, J. Chem. Phys. **87**, 1261 (1987)
47. N.V. Vargaftik, V.S. Yargin, A.A. Voshchinin, V.I. Dolgov, V.M. Kapitonov, N.I. Sidorov, Y.V. Tarlakov, High Temp. High Press **16**, 57 (1984)
48. F. Stepanko, N.I. Sidorov, Y.V. Tarlakov, V.S. Yargin, Int. J. Thermophys. **7**, 829 (1986)
49. D.L. Timrot, A.N. Varava, High Temp. **15**, 634 (1977)
50. N.V. Vargaftik, A.A. Voschchinin, High Temp. **5**, 715 (1967)
51. D.L. Timrot, V.V. Makhrov, V.I. Sviridenko, High Temp. **14**, 58 (1976)